INL/CON-14-31247
PREPRINT

INVESTIGATION OF A DYNAMIC POWER LINE RATING CONCEPT FOR IMPROVED WIND ENERGY INTEGRATION OVER COMPLEX TERRAIN

Proceedings of the ASME 2014 4th Joint US-European Fluids Engineering Division Summer Meeting and 11th International Conference on Nanochannels, Microchannels, and Minichannels FEDSM2014

Tyler B. Phillips, Inanc Senocak, Jake P. Gentle, Kurt S. Myers, Phil Anderson

August 2014

Proceedings of the ASME 2014 4th Joint US-European Fluids Engineering Division Summer Meeting and 11th International Conference on Nanochannels, Microchannels, and Minichannels
FEDSM2014
August 3-7, 2014, Chicago, Illinois, USA

FEDSM2014-21377

INVESTIGATION OF A DYNAMIC POWER LINE RATING CONCEPT FOR IMPROVED WIND ENERGY INTEGRATION OVER COMPLEX TERRAIN

Tyler B. Phillips
Boise State University
TylerPhillips1@u.boisestate.edu

Inanc Senocak
Boise State University
Senocak@boisestate.edu

Jake P. Gentle
Idaho National Laboratory
Jake.Gentle@inl.gov

Kurt S. Myers
Idaho National Laboratory
Kurt.Myers@inl.gov

Phil Anderson
Idaho Power Company
PAnderson2@idahopower.com

ABSTRACT

Dynamic Line Rating (DLR) is a smart grid technology that allows the rating of power line conductor to be based on its real-time temperature. Currently, conductors are generally given a conservative static rating based on worst case weather conditions. Using historical weather data collected over a test bed area in Idaho, we demonstrate there is often additional transmission capacity not being utilized under the current static rating practice. We investigate a DLR method that employs computational fluid dynamics (CFD) to determine wind conditions along transmission lines in dense intervals. Simulated wind conditions are then used to calculate real-time conductor temperature under changing weather conditions. In calculating the conductor temperature and then inferring the ampacity, we use both a steady-state and transient calculation procedure. Under low wind conditions, the steady-state assumption predicts higher conductor temperatures which could lead to unnecessary curtailments, whereas the transient calculations produce conductor temperatures that can be significantly lower, implying the availability of additional transmission capacity. Equally important, we demonstrate that capturing the wind direction variability in the simulations is critical in estimating conductor temperatures accurately.

INTRODUCTION

Transmission congestion is a growing concern that could limit integration of new renewable energy projects to the grid [1]. Transmission service providers (TSPs) are investigating alternative methods to increase transmission ampacity because construction of new power lines is a long and expensive process. Ampacity is the maximum electrical current a conductor can carry without exceeding its sag or annealing temperature limit. Wind speed and its direction relative to the power line are two major factors contributing to conductor temperature. Research has shown there is a strong connection between wind power output and transmission line ampacity [2]. When there is significant wind power production, local transmission lines are convectively cooled by the elevated winds. However, wind conditions can vary from high to low over complex terrain, which could create uncertainties when calculating the conductor temperature.

In current practice, TSPs generally use a static line rating (SLR) method to determine conductor ampacity. This approach can be very conservative, as it often assumes worst case weather conditions to avoid excessive conductor sag, ensuring public safety. DLR on the other hand, rely on real-time conductor temperature to determine ampacity. Dynamic ratings can be an economical and effective method to increase the electrical capacity of a conductor when favorable weather conditions permit.

Conductor temperature can vary significantly along its length due to the variation of weather conditions [3], especially in regions of complex terrain. Some of the DLR technologies used in industry today include direct line sag, line tension, and conductor temperature measurements [4]. Sag and tension systems only give the average sag or tension measurement over large sectionalized transmission spans, therefore, only the average conductor temperature over a given section is known. Direct temperature measurements are only taken at single fixed point locations. The concern with these systems is that they typically don't take enough measurements to give an accurate assessment of the varying conductor temperature [5], potentially leading to an over estimation of actual ratings [6]. Adding more monitoring devices could be a solution, however these systems are typically too expensive, requiring many instruments to reduce error to an acceptable level [7]. Equally important, implementation of direct measurement systems can prove to be challenging, as transmission lines may need to be de-energized during installation.

Idaho National Laboratory (INL), with funding from the Department of Energy through the Wind and Water Power Technology Office, and Idaho Power Company (IPCo) are researching a database approach of pre-computed CFD simulations to dynamically rate transmission lines [5, 7–9]. They are using WindSim CFD software, with conventional 3-D Reynolds-Averaged Navier-Stokes equations and the standard k-ε turbulence model for steady-state simulations. They take into account land topography, surface roughness of the terrain, and wind conditions at 17 weather stations over their test area. The simulations are computationally too intensive to be done in real-time. Therefore, real-time weather station measurements are used to lookup a pre-computed simulation that best resembles the current wind conditions. They are then applied along the transmission line and the real-time ampacity is calculated using the IEEE (Institute of Electrical and Electronics Engineers) steady-state thermal rating equation. It is believed in most situations the error from using a steady-state equation is likely to be small, but recognized in [9] that under highly variable weather conditions transient equations may be desired. In this study we address the steady-state procedure using transient calculations and demonstrate the marked difference on real-time temperature calculations.

In this paper, we describe our efforts toward developing a new DLR method that takes into account the transient response of conductor temperature. When local weather conditions are available in near real-time, a transient calculation allows us to more accurately calculate conductor temperature, especially during times of rapidly changing weather conditions. Additionally, we investigate the applicability of a GPU-accelerated wind forecasting approach [10–12] to predict wind conditions along the path of transmission lines. It's expected that a transient calculation approach will give a more accurate representation of conductor temperature, which could enable TSPs to transfer wind farm generation more efficiently and reliable.

IEEE STANDARD 738-2006

In engineering practice, overhead power line ampacity is commonly calculated using one of the two standards; the IEEE 738 [13], or the Conseil International des Grands Reseaux Electriques (CIGRE) [14]. Both standards follow the same concept, the balance of the heat equation, illustrated in Fig. 1. Conductor temperature is a function of their materials, physical properties, weather conditions, and the electrical current. The IEEE steady-state heat balance equation is given as

$$q_c + q_r = q_s + q_j \tag{1}$$

where q_c is the conductor convective heat loss, q_r is the conductor radiated heat loss, q_s is the conductor solar heat gain and q_j is the Joule heating.

The Joule heating is determined by the electric current, I, and the resistance, R, at a given conductor temperature, T_c. The Joule heating is given as

$$q_j = I^2 R(T_c) \tag{2}$$

Equations (1) and (2) are combined, giving the steady-state thermal rating, which is expressed as

$$I = \sqrt{\frac{q_c + q_r - q_s}{R(T_c)}} \tag{3}$$

This equation is used to calculate the steady-state ampacity by assuming the resistance of conductor at maximum permissible temperature. It is used in the DLR calculation procedure described in [5, 7–9].

The rate of solar heating and radiative cooling is defined as follows, respectively

$$q_s = \alpha Q_{se} \sin(\theta) A' \tag{4}$$

$$q_r = 0.0178 D \varepsilon \left[\left(\frac{T_c + 273}{100} \right)^4 - \left(\frac{T_a + 273}{100} \right)^4 \right] \tag{5}$$

Here α, Q_{se}, θ, A', T_a, D and ε are the solar absorptivity of the conductor, total corrected solar radiated heat flux, effective angle of incidence of the sun, projected area of conductor per unit length, ambient temperature, conductor diameter, and conductor emissivity, respectively.

The convective cooling is defined depending on the wind velocity. For zero, low, and high wind velocity, convective

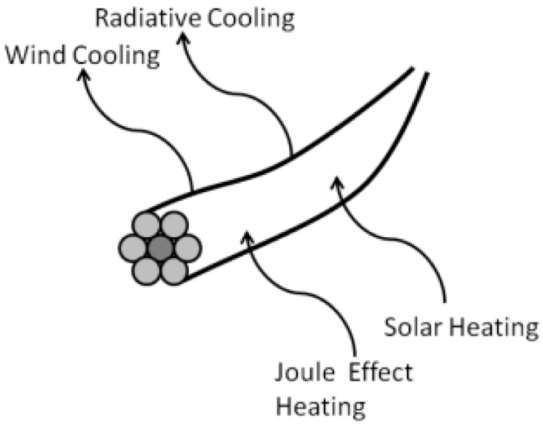

FIGURE 1. DIAGRAM OF THE HEAT BALANCE WITHIN A CONDUCTOR [9].

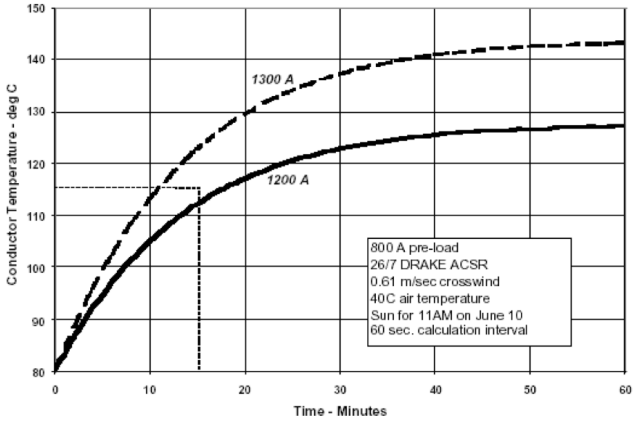

FIGURE 2. TRANSIENT TEMPERATURE RESPONSE TO A STEP CHANGE IN CURRENT. GRAPH ADOPTED FROM [13].

cooling is defined as follows, respectively

$$q_{c_n} = 0.0205 \rho_f^{0.5} D^{0.75} (T_c - T_a)^{1.25} \tag{6}$$

$$q_{c_1} = \left[1.01 + 0.0372 \left(R_{e_D}\right)^{0.52}\right] k_f \; K_{angle} (T_c - T_a) \tag{7}$$

$$q_{c_2} = 0.0119 \left(R_{e_D}\right)^{0.6} k_f \; K_{angle} (T_c - T_a) \tag{8}$$

In the above equations ρ_f, k_f, K_{angle}, and R_{e_D} are the air density, thermal conductivity of air, wind direction factor, and the Reynolds number around a cylinder, respectively. For wind speed above zero, forced convection is determined by using the largest of q_{c_1} and q_{c_2}.

In practice, conductor temperature is constantly changing in response to changing electrical current and weather conditions (Fig. 2). This transient response can be modeled as a first order differential equation (ODE), which can be solved by employing numerical methods, it is expressed as

$$\frac{dT_c}{dt} = \frac{1}{mC_p} \left[q_j + q_s - q_c - q_r\right] \tag{9}$$

where mC_p is the total heat capacity of the conductor. The calculated heat capacity is given as

$$mC_p = \sum m_i C_{pi} \tag{10}$$

where m_i and C_{pi} are the mass per unit length of i^{th} conductor material and the specific heat of i^{th} conductor material, respectively. The DLR method described in this paper employs a 4^{th} order Runge-Kutta method to solve the transient ODE, determining the real-time conductor temperature.

VALIDATION OF CONDUCTOR TRANSIENT RESPONSE AND STEADY-STATE TEMPERATURE

Bontempi et al. [15] suggested the convective heat transfer correlations in the IEEE standard could be improved. Therefore, CFD simulations were completed using ANSYS FLUENT to validate IEEE steady-state and transient conductor temperature equations. Starling 26/7 ACSR (aluminum conductor steel reinforced) was modeled as two concentric cylinders, aluminum with a steel core. Only convective cooling was considered, solar heating and radiative losses were set to zero for both CFD simulations and IEEE calculations. Joule heating is applied as a heat generation term in the aluminum region where 98–99% of the current is carried in ACSR conductor [16].

Three high quality 2D structured computational meshes consisting of 23,820 nodes were created using ICEMCFD. All three meshes consist of the same number of cells, only the size of the cell-adjacent to the conductor is changed, allowing the wall-adjacent cell centroid to lie in the log-law layer under different wind velocity. The cell-adjacent centers should be located a sufficient distance away from the wall, consistent with the standard wall-function formulation. The lower limit lies in the order of $y^+ \sim 15$, below this the wall functions will typically deteriorate and the accuracy of the solution cannot be maintained [17].

Steady-state simulations were completed with a laminar flow model, where wind velocity ranged between 0.5–3m/s, orthogonal to the conductor axis. The standard k-ε turbulence model, with a standard wall-function, was employed for wind

velocity ranging from 2–10m/s. Both models were used in the transition region, 2–3m/s, where the Reynolds numbers based on conductor diameter is ∼3,100 and ∼4,700, respectively. Steady-state results are shown in Fig. 3, the small, medium, and large wall cell refers to the size of the cell-adjacent to the conductor. CFD results and IEEE calculations are in general agreement, with CFD results giving lower conductor temperature with wind speed above 5m/s.

Transient CFD simulations were completed at laminar (1m/s) and turbulent (8m/s) wind velocity orthogonal to the conductor. The transient time step size used in simulations was sufficiently small to accurately capture the vortex shedding created in the wake of the conductor. The IEEE transient ODE, Eq. (9), was calculated using MATLABs built in ode45 solver, which maintains relative and absolute tolerances of 1E-3 and 1E-6 [18], respectively. Simulation results and IEEE calculations were plotted and the results overlapped one another.

Theses CFD validations instill further confidence in the use of IEEE Standard 738 equations in a computationally based DLR technology. Furthermore, the IEEE transient ODE was shown to accurately govern how a conductor temperature changes in time.

IDAHO NATIONAL LABORATORY & IDAHO POWER TEST BED

Significant wind power generation projects in southern Idaho have increased interest in DLR implementation. Because of the natural synergy between wind power generation and conductor convective cooling, it is desired that when the wind blows, resulting in higher wind power generation, lines can be dynamically rated higher than the current SLR practice allows.

The INL/IPCo joint test bed area for DLR research is located on the Snake River Plain in southern Idaho. The test site covers an area approximately 1,500km^2 of moderately complex terrain. It consists of small towns, large farmland, and high desert mountainous terrain. Elevation of the test site ranges from approximately 754−1,198m, the land topology, transmission lines, and weather stations are shown in Fig. 4.

Seventeen weather stations have been mounted in strategic locations along more than 190km of high-voltage transmission lines. Weather stations are spaced between 1.5 and 8km, at a height of 10m above ground level. The measured quantities are wind speed, wind direction, ambient temperature, and solar irradiation. Data from the weather stations is collected every 3 minutes, it is an average of 2-second readings over the 3-minute time interval. Measurements started in August of 2010 and are currently ongoing as of May 2014.

INL & IPCo Test Bed Ampacity Ratings Analysis

Transmission line ampacity is limited by the critical span, or segment resulting in the highest conductor temperature, often

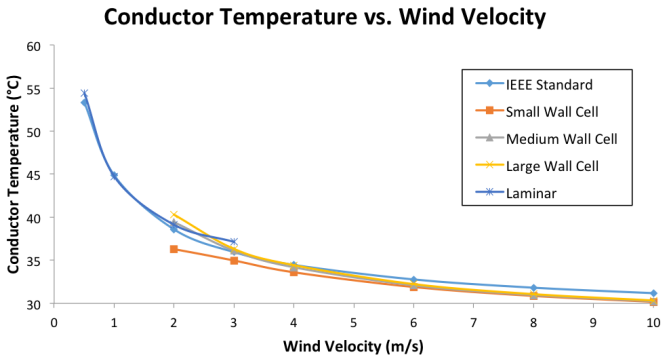

FIGURE 3. VALIDATION OF IEEE STANDARD 738 STEADY-STATE CONDUCTOR TEMPERATURE. SMALL, MEDIUM, AND LARGE WALL CELL REFERS TO THE SIZE OF THE CELL-ADJACENT TO THE CONDUCTOR.

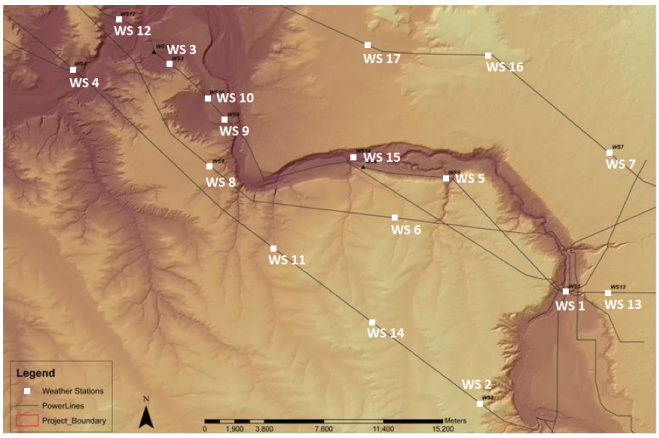

FIGURE 4. INL/IPCo TEST BED AREA FOR DLR RESEARCH. ADAPTED FROM [7].

the segment experiencing the lowest wind velocity. The DLR analysis in this paper uses year-long weather data from weather station 17 (WS17) starting July 1, 2012. WS17 had lower wind velocity than other weather stations along the transmission line investigated, therefore selected. This doesn't imply that it is the limiting section at all times, it's only statistically the most likely limiting section. Sections of transmission lines that are routinely the critical span may be replaced with a higher ampacity conductor to "balance" the ratings along a transmission line.

In this analysis, ampacity of Starling 26/7 ACSR conductor has been calculated seasonally as follows; spring (Mar-May), summer (Jun-Aug), fall (Sep-Nov) and winter (Dec-Feb). Starling conductor does not represent actual transmission lines across the test area. The transmission line at WS17 is assumed to run in the WNW–ESE direction, have real-time maximum solar heat-

ing, and a maximum allowable temperature of 75°C. Seasonal real-time ampacity results are shown in Fig. 5. The horizontal dashed line represents the SLR of 849 Amps, given by Southwire [19]. Southwire ratings are calculated assuming a 75°C maximum conductor temperature, 0.61m/s wind velocity, and 25°C ambient temperature under sun. The solid lines represent the 10^{th} (bottom line) through 90^{th} (top line) real-time ampacity percentile. The percentile is a measure used in statistics indicating the value below which a given percentage of observations occur. For example, the 20^{th} percentile is the ampacity value which 20% of the ampacity observations fall below.

It's clear that SLRs are limiting transmission capacity at this location, especially during times of elevated wind velocity, when large local wind generation is expected and additional capacity is desired. The lowest ampacity occurs during the summer, when high ambient temperature and low wind velocity exist. Even under these unfavorable conditions, only the 10^{th} percentile falls below the static rating around midnight, when wind velocity drops to zero. In general, each season exhibits over a 70% increase in ampacity half of the time, and a 20% increase 90% of the time.

However, the above discussion is limited to a local observation at a point. We are interested in implementing DLR over a large area, therefore we need to know the spatial variation of wind speed.

CFD-BASED WIND MODELING OVER COMPLEX TERRAIN

Numerical weather prediction models have been used to forecast winds, however their applicability to micro-scale atmospheric boundary layer flows and ability to reliably predict wind speeds within the surface layer is not clear. In this study, we use a multi-GPU (graphics processing unit) parallel wind solver, which has been under continuous development at Boise State University since 2007 [10–12, 20, 21], to potentially forecast winds over arbitrarily complex terrain at the micro-scale. Computational domain size can range from meters to several kilometers. The computations are accelerated on GPU clusters with a dual-level parallel implementation that interleaves Message Passing Interface with NVIDIA's Compute Unified Device Architecture. The overall goal for the solver is to forecast micro-scale atmospheric flows over complex terrain.

In the wind solver, a hybrid RANS-LES technique [22] that blends the Lagrangian dynamic subgrid-scale model [23] with the Prandtl's mixing length model is used for turbulence closure. The Lagrangian dynamic model is a localized model and does not require any homogeneous directions in the computational domain, therefore is adequate for arbitrarily complex terrain. In the solver, a Cartesian immersed boundary method is used to impose boundary conditions on the surface using logarithmic reconstructions [24]. Additionally, the Cartesian mesh method maps well to the computer architecture of GPUs, allowing for efficient parallel computing.

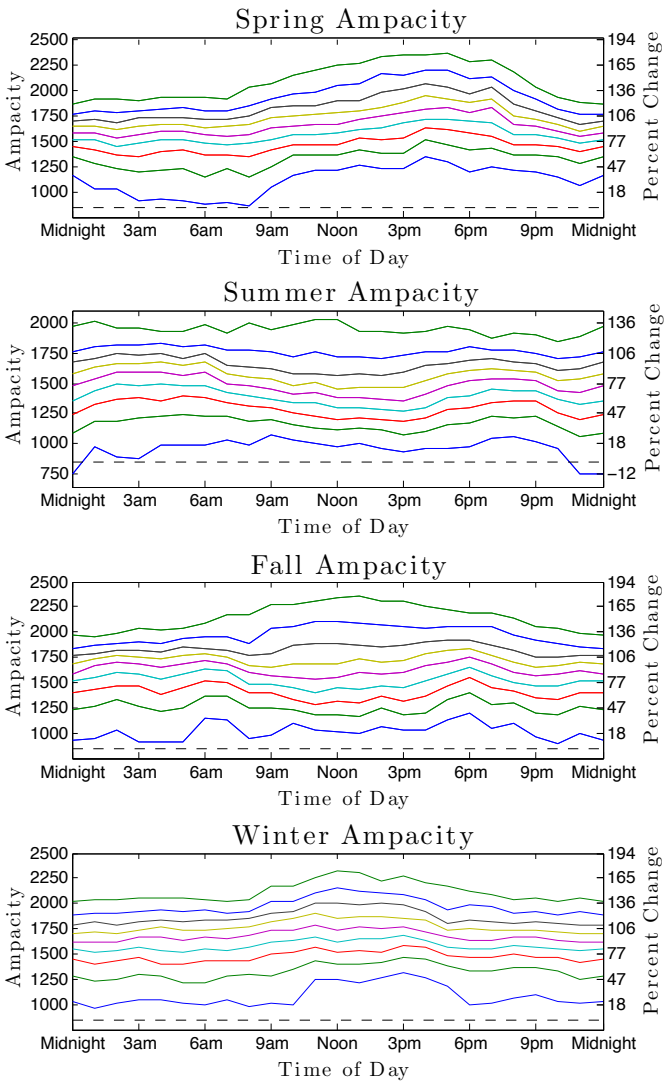

FIGURE 5. SEASON HOURLY AMPACITY PERCENTILE USING REAL-TIME WEATHER CONDITIONS. SOLID HORIZONTAL LINES REPRESENT THE 10–90 PERCENTILE FROM BOTTOM TO TOP, RESPECTIVELY. THE HORIZONTAL DASHED LINE REPRESENTS THE SOUTHWIRE STATIC RATING (849 A) [19].

CFD Simulation Results

Prevailing winds across the test bed location are in the east and west direction. The wind solver was therefore ran with periodic boundary conditions with a forcing that produce a wind flow across the terrain with a general magnitude of $\sim$ 5.5m/s at a height of 10m above ground level, out of the west. The wind

speed at a height of 10m is shown by the velocity contour in Fig. 6.

Initial attempts to assess the wind flow solver results have been done by comparing CFD wind velocity to real-time weather station measurements. It's recognized that this is a difficult and incomplete task, as the current state of the wind solver does not permit time-dependent turbulent lateral boundary conditions. The current neutral stability assumption is also far from the reality of convective turbulence over the complex terrain. We also note that point-wise weather station data can be highly influenced by local variations in the terrain which may be missing in the simulations. Therefore, we deem our assessment of simulation results as preliminary at this stage.

In light of these reservations, the mean wind speed of 27 discrete hour-long real-time measurements, which best represent or mimic the CFD boundary conditions have been selected for comparison. Each discrete hour-long mean wind speed is calculated using real-time wind data, which is sampled at 3 minute time intervals. The mean and standard deviation of the 27 discrete hour-long measurements is compared with CFD results, shown in Fig. 7. Weather stations 7, 12, and 13 did not fall in the domain of the wind solver, and therefore are excluded.

Simulated wind speed at eight of the fourteen weather stations match real-time measurements rather well, however, six fall outside the standard deviation. At this time, it is unclear if this is due to the developmental stage of the flow solver, or digitization of the weather station location which was done utilizing Fig. 4. In regions of complex terrain, wind can dramatically change within a few meters, because of local effects that may not be present in the simulations. For instance, weather stations 3, 5, and 15 are located in regions of complex terrain, were small variations in position can have a large effect on wind speed. Additionally weather station 14 data has been deemed deficient.

Wind velocity is extracted along the length of transmission lines at ∼6,400 locations. Using the extracted wind velocity the steady-state conductor temperature is calculated assuming a constant load of 849 Amps, 35°C ambient temperature, 12 W/m solar heating, and Starling 26/7 ACSR conductor, which does not represent actual IPCo transmission lines. Conductor temperature is superimposed with the land topography, shown in Fig. 8. Spatial temperature difference along the four transmission lines can be seen in Fig. 9.

The effect of wind speed and its direction is clearly visible by the spatial conductor temperature over the test area. The conductor temperature along transmission lines 1–4 ranges by 23.5, 38.5, 48.1, and 20.9°C, respectively. Elevated conductor temperature exist where wind direction is parallel to the transmission lines, and in regions of complex terrain conductor temperature can be significantly higher due to much lower wind velocity. Clearly in areas of complex terrain, conductor temperature must be determined in highly dense intervals to resolve the spatial temperature changes.

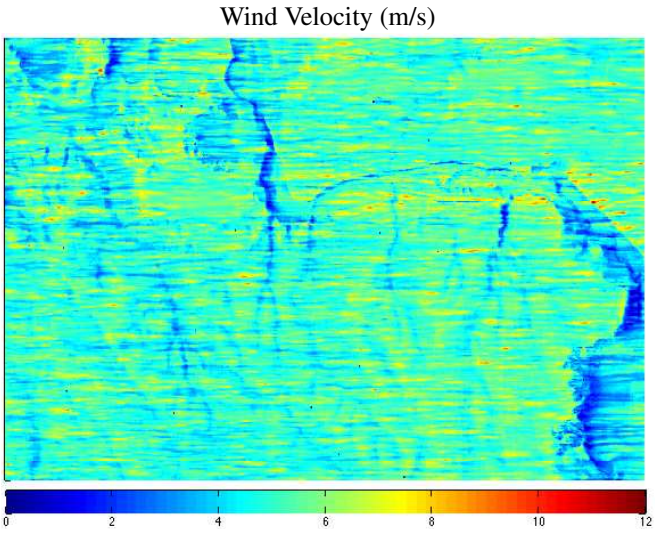

FIGURE 6. WIND CONTOUR AT 10 METERS ABOVE THE GROUND LEVEL.

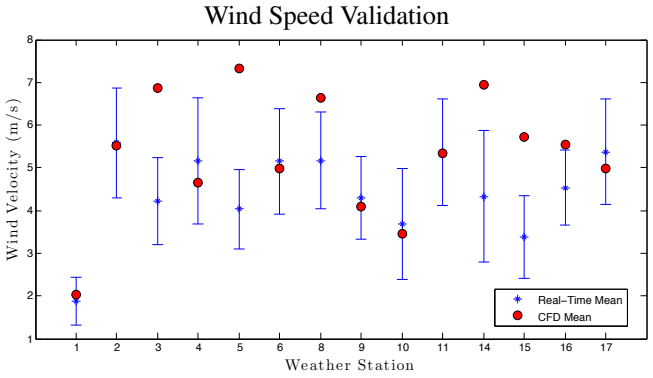

FIGURE 7. COMPARISON AT WEATHER STATION LOCATIONS OF CFD TO REAL-TIME MEAN AND STANDARD DEVIATION OF 27 DISCRETE HOUR LONG MEASUREMENTS DURING THE SUMMER.

DLR METHODOLOGY USING A TRANSIENT CONDUCTOR APPROACH

The DLR method described in [5,7–9] calculates the dynamically changing real-time conductor ampacity using the IEEE steady-state thermal rating, Eq. (3). It is believed that in most situations the error from assuming steady-state is likely to be small, but recognized that under highly variable local weather conditions transient equations may be desired [9].

In the present effort, we determine the conductor temperature by calculating the transient thermal response of a conductor due to changing weather conditions. A transient approach is favored, as it gives a more realistic representation of changing conductor temperature, especially when rapidly changing weather or

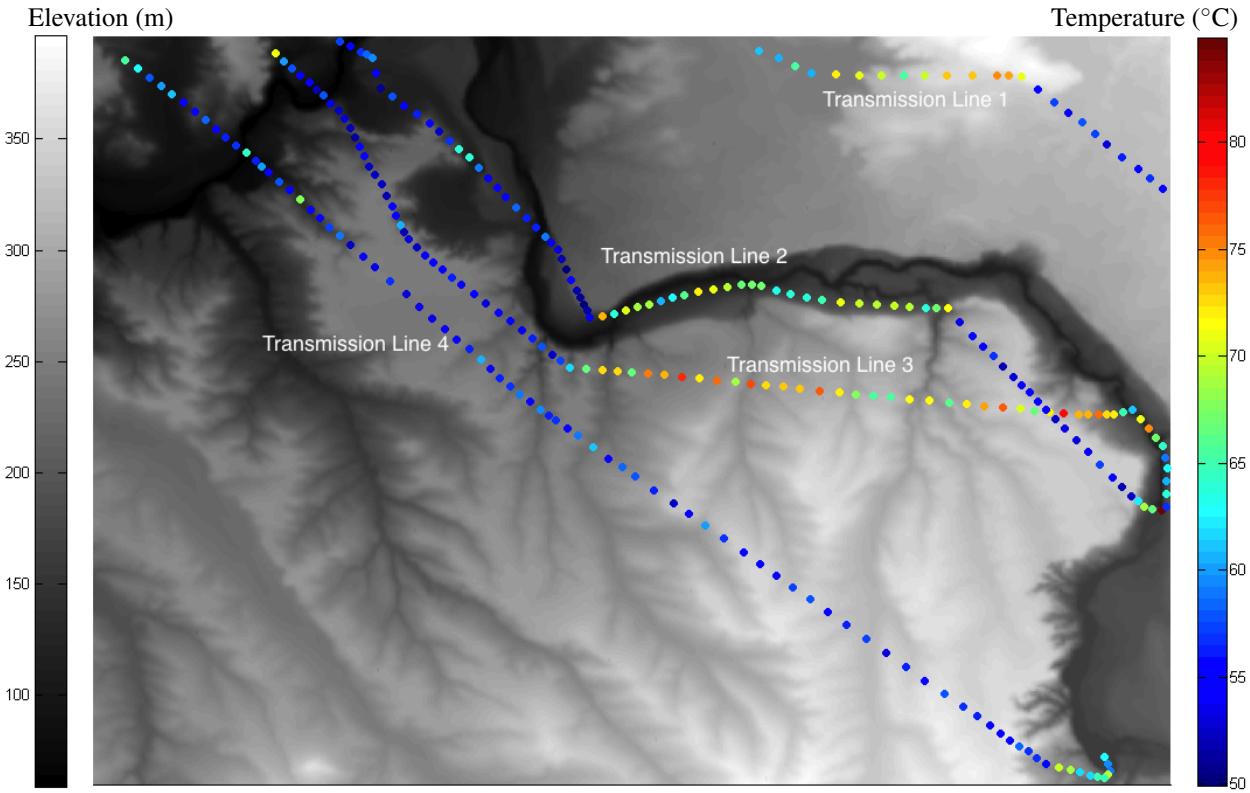

FIGURE 8. CONDUCTOR TEMPERATURE SUPERIMPOSED WITH LAND TOPOGRAPHY.

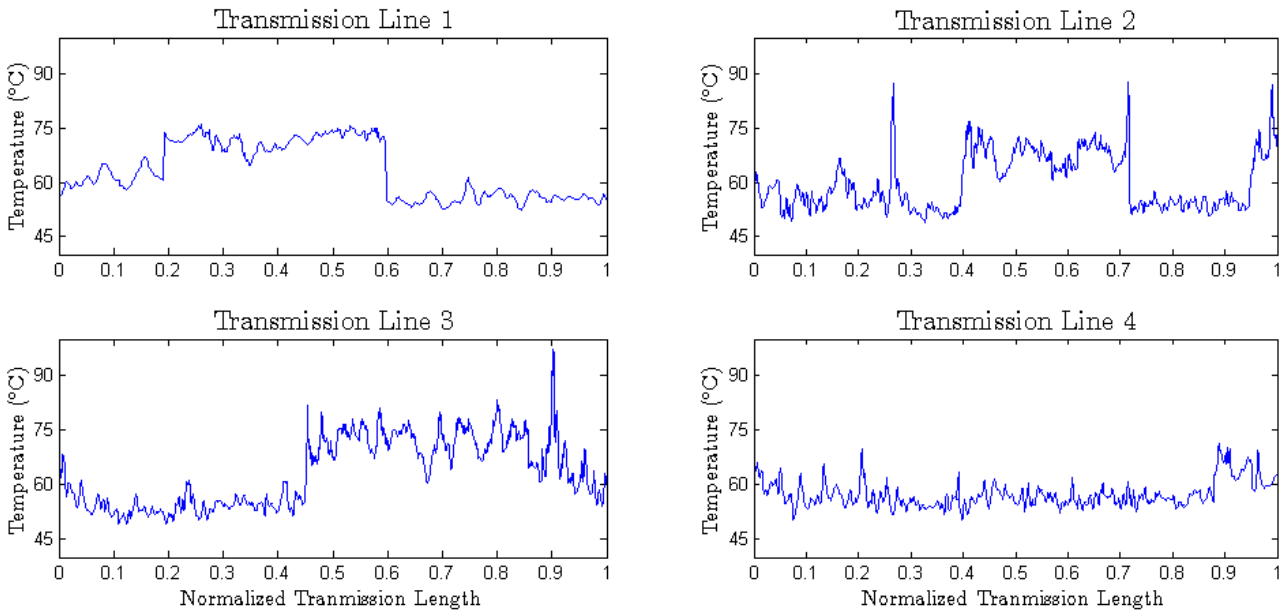

FIGURE 9. SPATIAL VARIATION OF CONDUCTOR TEMPERATURE ALONG TRANSMISSION LINES.

electrical loading conditions occur. Due to a conductor's heat capacity, its temperature does not exhibit an instantaneous thermal response to changing conditions, unlike what is implied by the steady-state calculation procedure. A transient calculation approach within a DLR method takes advantage of the the heat capacity of the conductor and its initial temperature, which may reduce curtailment on transmission conductor.

It should be noted that it is not possible to directly compare the steady-state DLR method discussed in [5, 7–9], and the transient approach discussed in this paper. The steady-state procedure calculates the real-time IEEE steady-state thermal rating equation, Eq. (3), which solves the maximum current a conductor can undergo while staying within its thermal limit, by assuming a maximum allowed conductor temperature.

A transient method, calculates the real-time conductor temperature, using real-time weather and electrical loading conditions. Therefore, to compare steady-state and transient calculations, a constant electrical current is applied and the steady-state conductor temperature is then inferred using the conductor resistance, which is given as

$$R(T_c) = \frac{q_c + q_r - q_s}{I^2} \tag{11}$$

After knowing the resistance, the steady-state conductor temperature is extracted from tabulated data of resistance versus temperature using a linear interpolation.

Real-time weather data with a constant load of 849 Amps, applied to both steady-state and transient equations, is used for this test case scenario. The top plot in Fig. 11 shows the real-time steady-state ampacity, assuming a maximum thermal limit of 75°C. The bottom plot shows the comparison of steady-state and transient conductor temperature calculations. Unlike the steady-state calculation, the transient method does not undergo instantaneous changes in temperature with changing weather conditions. Essentially, the heat capacity creates a "dampening" affect for the temperature response.

During times of high wind velocity, the calculated steady-state and transient temperature show little difference. However, when low wind velocity occurs, the steady-state calculation undergo an instantaneous conductor temperature change that can exceed the conductor thermal limit. Only when the initial temperature of conductor is high or the unfavorable conditions persist over an extended time period, does the actual conductor temperature given by the transient calculation exceed the thermal limit. When emergency conditions do arise, overhead conductors may be operated at higher temperature ratings. ACSR is not a high-temperature conductor, it is rated for 75°C continuous operation, but may be operated at emergency temperature ratings up to 100°C for a total of 1,500 hours over the conductor life [19].

Emergency and curtailment conductor temperatures are compared using real-time season long weather data. Weather data from the summer is applied to both steady-state and transient temperature equations. Again, a constant load of 849 Amps and real-time maximum solar heating is applied. Temperature results between steady-state and transient calculation procedures are shown in Fig. 10. In general, both steady-state and transient temperatures are similar. However, the steady-state calculation result in temperature calculations which would indicate curtailment (> 100°C) four times as often as the transient calculation, 111 vs. 27 hours.

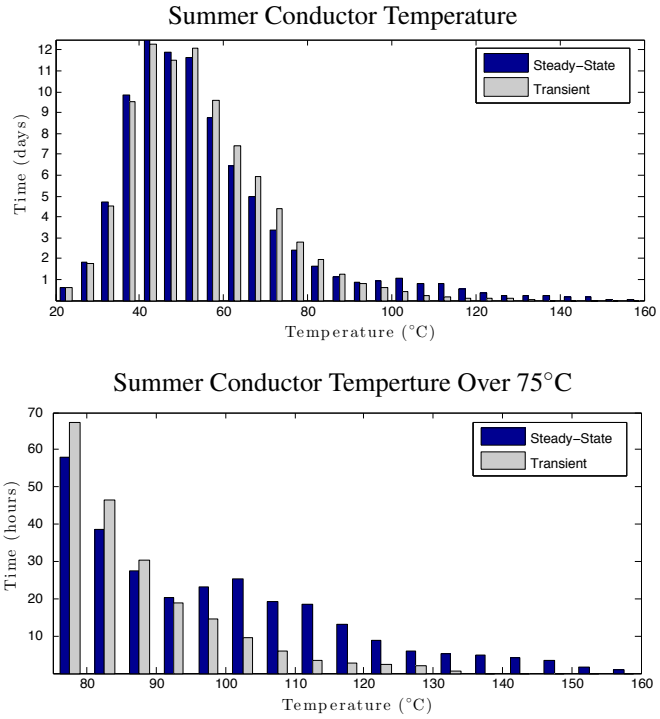

FIGURE 10. TOP: SUMMER CONDUCTOR TEMPERATURE USING STEADY-STATE AND TRANSIENT PROCEDURE OVER A PERIOD OF 88 DAYS. BOTTOM: COMPARISON OF CONDUCTOR TEMPERATURES THAT INDICATE EMERGENCY RATINGS OR CURTAILMENT.

SUMMARY AND FUTURE WORK

Using historical weather data from a test bed in Idaho, we have shown the conventional SLR practice is often times limiting transmission line capacity. Our analysis of the INL/IPCo test bed area indicates DLR can increase electrical capacity by 20% over 90% of the time, and by 70% half of the time. We have presented our efforts towards developing a new computationally based DLR method that calculates conductor temperature utilizing the transient ODE model. It was shown that the ODE model

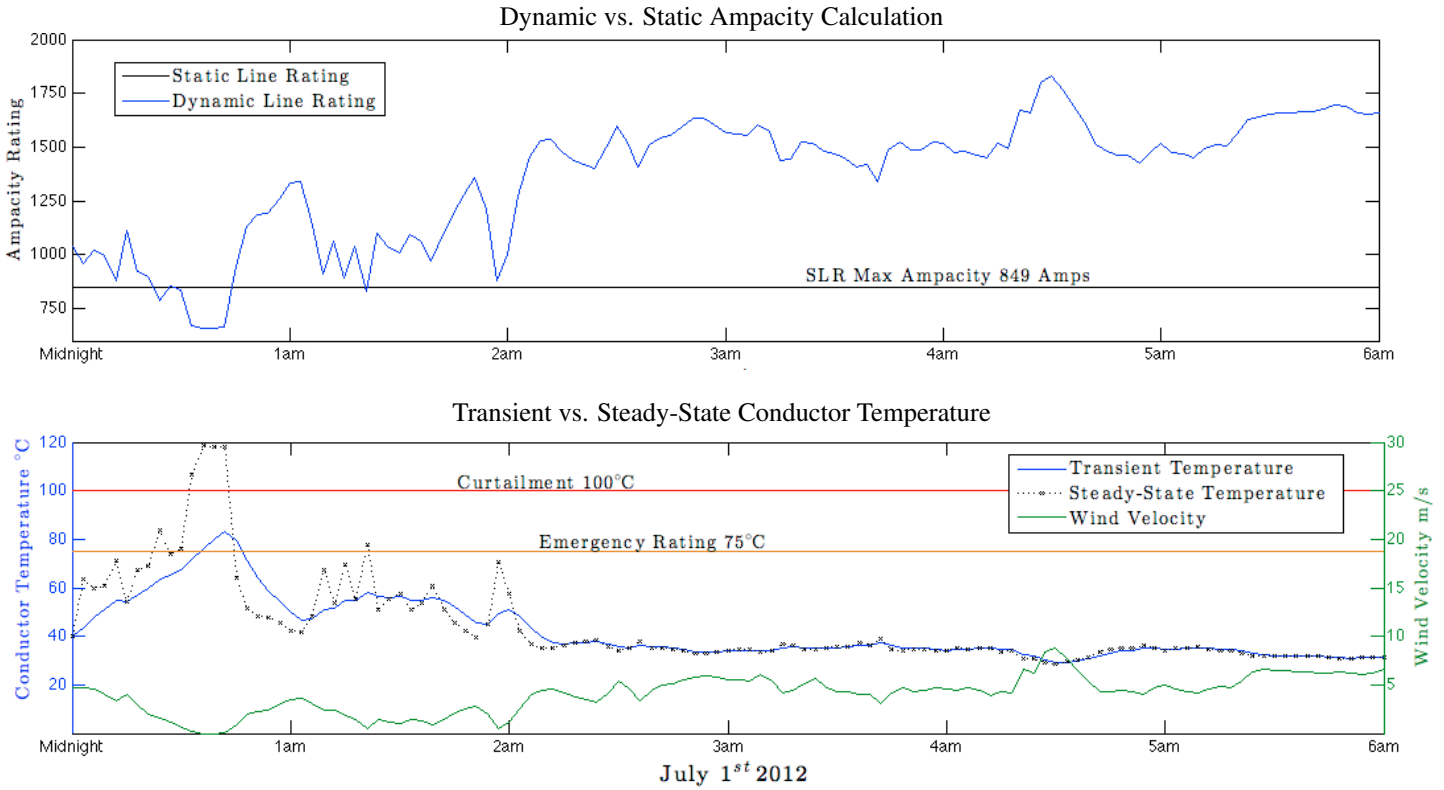

FIGURE 11. TOP: STATIC AND DYNAMIC REAL-TIME AMPACITY CALCULATION. BOTTOM: COMPARISON OF STEADY-STATE AND TRANSIENT CONDUCTOR TEMPERATURE CALCULATION.

accurately governs conductor temperature change in time due to changing weather or electrical conditions. A transient approach should be favored, as it allows us to better calculate the real-time conductor temperature than the steady-state method used in other studies. We have demonstrated using both steady-state and transient calculation methods that under low wind speed conditions, steady-state calculations predict higher conductor temperatures that could lead to unnecessary curtailment of power transmission, whereas the transient calculations produce results in conductor temperature that are significantly lower, implying the availability of additional transmission capacity, avoiding unnecessary curtailments. Additionally, we have shown that capturing the wind direction across the domain is important, as wind direction relative to the transmission lines plays a dominant role in estimating the conductor temperature. Its expected our computational approach will help TSPs transfer power generation with increased capacity.

GPU-accelerated wind field computations over complex terrain that are presented in this paper are promising but deemed preliminary, because the current state of the solver does not address time-dependent lateral boundary conditions and thermal stability of the atmosphere. Work is in progress to incorporate these features into the solver. The focus of our ongoing and future work will be to incorporate the necessary physical models into the solver, evaluate wind simulations using wind measurements, perform a grid refinement study, and produce a systematic analysis of both solution accuracy and computational performance of our flow solver.

ACKNOWLEDGMENTS

This research has been partially funded by grants from the National Science Foundation (Award Nos. 1056110 and 1229709). Authors would like to thank Micah Sandusky and Rey DeLeon for their help in generating the CFD simulation.

REFERENCES

[1] Schell, P., Lambin, J., Godard, B., Nguyen, H., and Lilien, J., 2011. "Using Dynamic Line Rating to Minimize Curtailment of Wind Power Connected to Rural Power Networks". Proceedings of the 10^{th} International Workshop on Large-Scale Integration of Wind Power into Power Systems.

[2] Belben, P., and Ziesler, C., 2002. "Aeolian Uprating: How Wind Farms Can Solve Their Own Transmission Prob-

lems". In Proceedings of 1st World Wind Energy Conference and Exhibition.

[3] EPRI, 2005. "Increased Power Flow Guidebook: Increasing Power Flow in Transmission and Substation Circuits". Palo Alto, CA. 1010627.

[4] Uski-Joutsenvuo, S., Pasonen, R., and Rissanen, S., 2012. "Maximising Power Line Transmission Capability by Employing Dynamic Line Ratings: Technical Survey and Applicability in Finland".

[5] Gentle, J. P., Myers, K. S., Bush, J. W., and Carnohan, S. A., 2013. "Dynamic Line Rating Systems in the U.S.: Policy and Reliability". INL/EXT-13-28553.

[6] Seppa, T. O., Mohr, R. D., and Stovall, J., 2010. "Error Sources of Real-Time Ratings Based on Conductor Temperature Measurements". Report to CIGRE WG B2.36, Stockholm, Sweden. pp. 20–21.

[7] Gentle, J., Myers, K. S., Baldwin, T., West, I., Hart, K., Savage, B., Ellis, M., and Anderson, P., 2012. INL/CON-12-27012. "Concurrent Wind Cooling in Power Transmission Lines". In 2012 Western Energy Policy Research Conference.

[8] Gentle, J. P., Myers, K. S., West, I. J., Anderson, P., Hart, K., and Ellis, M., 2012. "Wind Modeling to Predict Cooling in Transmission Lines". Idaho National Labratory.

[9] Greenwood, D. M., Gentle, J. P., Ingram, G. L., Davison, P. J., Myers, K. S., West, I. J., Bush, J. W., and Troffaes, M. C., 2014. "A Comparison of Real Time Thermal Rating Systems in the U.S. and the UK". IEEE Transactions on Power and Delivery.

[10] DeLeon, R., Felzien, K., and Senocak, I., 2012. "Toward a GPU-Accelerated Immersed Boundary Method for Wind Forecasting Over Complex Terrain". ASME 2012 Fluids Engineering Division Summer Meeting, ***1***, July 8–12.

[11] Jacobsen, D. A., and Senocak, I., 2013. "Multi-level Parallelism for Incompressible Flow Computations on GPU Clusters". Parallel Computing, ***39***(1), pp. 1 – 20.

[12] Thibault, J. C., and Senocak, I., 2012. "Accelerating Incompressible Flow Computations With a Pthreads-CUDA Implementation on Small-footprint Multi-GPU Platforms". Journal of Supercomputing, ***59***(2), pp. 693–719.

[13] IEEE, 2007. "IEEE Standard 738: Calculation the Current-Temperature of Bare Overhead Conductors".

[14] CIGRE, 1992. "The thermal behaviour of overhead conductors". CIGRE WG 12.

[15] Bontempi, G., Vaccaro, A., and Villacci, D., 2008. "Data-driven Calibration of Power Conductors Thermal Model for Overhead Lines Overload Protection". International Journal of Reliability and Safety, ***2***(1), pp. 5–18.

[16] Clairmont, B., Douglass, D., Inglesias, J., and Peter, Z., 2012. Radial and Longitudinal Temperature Gradients in Bare Stranded Conductors with High Current Densities. Tech. Rep. CIGRE B2-108, Paris.

[17] ANSYS, Inc., 2011. "ANSYS Fluent 14.0: Theory Guide". Canonsburg, PA,

[18] The Math Works, Inc. "MATLAB Release 2012a". Massachusetts, United States.

[19] Southwire Company, 2007. "Overhead Conductor Manual". Carrollton, Ga.

[20] Jacobsen, D. A., and Senocak, I., 2011. "A Full-Depth Amalgamated Parallel 3D Geometric Multigrid Solver for GPU Clusters". In 49th AIAA Aerospace Science Meeting, no. AIAA-2011-946.

[21] DeLeon, R., Jacobsen, D., and Senocak, I., 2013. "Large-Eddy Simulations of Turbulent Incompressible Flows on GPU Clusters". Computing in Science and Engineering, ***15***(1), pp. 26–33.

[22] Senocak, I., Ackerman, A., Kirkpatrick, M., Stevens, D., and Mansour, N., 2007. "Study of Near-surface Models for Large-eddy Simulations of a Neutrally Stratified Atmospheric Boundary Layer". Boundary-Layer Meteorology, ***124***, pp. 405–424.

[23] Meneveau, C., Lund, T., and Cabot, W., 1996. "A Lagrangian Dynamic Subgrid-scale Model of Turbulence". Journal of Fluid Mechanics, ***319***, pp. 353–385.

[24] Senocak, I., Ackerman, A., Stevens, D., and Mansour, N., 2004. "Topography Modeling in Atmospheric Flows Using the Immersed Boundary Method". In Annual Research Briefs. Center for Turbulence Research, NASA-Ames/Stanford Univ., Palo Alto, CA, pp. 331–341.